Anthropogenic Aerosols Significantly Reduce Mesoscale Convective System Occurrences and Precipitation over Southern China in April

Lijuan Zhang[1], Tzung-May Fu[2,3,*], Heng Tian[1], Yaping Ma[1], Jen-ping Chen[4,5], Tzu-Chin Tsai[4], I-Chun Tsai[6], Zhiyong Meng[1], Xin Yang[2,3]

[1] Department of Atmospheric and Oceanic Sciences, School of Physics, Peking University, China

[2] School of Environmental Science and Engineering, Southern University of Science and Technology, Shenzhen, Guangdong Province, China

[3] Shenzhen Institute of Sustainable Development, Southern University of Science and Technology, Shenzhen, Guangdong Province, China

[4] Department of Atmospheric Sciences, National Taiwan University, Taiwan

[5] International Degree Program in Climate Change and Sustainable Development, National Taiwan University, Taiwan

[6] Research Center for Environmental Changes, Academia Sinica, Taiwan

* Corresponding author: Tzung-May Fu (fuzm@sustech.edu.cn)

Key Points:

- Anthropogenic aerosols inhibit mesoscale convective systems and reduce convective precipitation over Southern China in April
- Aerosols directly scatter solar radiation and indirectly exert Twomey effect on warm clouds to stabilize regional atmosphere

Abstract

Precipitation over Southern China in April, largely associated with mesoscale convective systems (MCSs), has declined significantly in recent decades. It is unclear how this decline in precipitation may be related to the concurrent increase of anthropogenic aerosols over this region. Here, using observation analyses and model simulations, we showed that increased levels of anthropogenic aerosols can significantly reduce MCS occurrences by 21% to 32% over Southern China in April, leading to less rainfall. Half of this MCS occurrence reduction was due to the direct radiative scattering of aerosols and the indirect enhancement of non-MCS liquid cloud reflectance by aerosols, which stabilized the regional atmosphere. The other half of the MCS occurrence reduction was due to the microphysical and dynamical responses of the MCS to aerosols. Our results demonstrated the complex effects of aerosols on MCSs via impacts on both the convective systems and on the regional atmosphere.

Plain Language Summary

Rainfall over Southern China for the month of April has decreased significantly between the late 1970s and the late 2000s, concurrent with increasing anthropogenic aerosol pollution in this region. Through model simulations, we found that higher levels of aerosols and the resulting increase in liquid cloud reflectance both enhanced the scattering of sunlight, cooled the surface, and stabilized the lower atmosphere. As a

result, the occurrences of strong, well-organized convective systems were suppressed, leading to decreased rainfall over Southern China in April.

1 Introduction

Atmospheric aerosols affect cloud systems and precipitation in complex ways [*Stevens and Feingold*, 2009; *IPCC*, 2013; *Fan et al.*, 2016; *Li et al.*, 2019]. Aerosols may scatter and/or absorb radiation to exert direct radiative forcing to the atmosphere and the surface, perturbing atmospheric stability [*Hansen et al.*, 1997]. Aerosols may also serve as cloud condensation nuclei (CNN) and ice nuclei (IN) and change the microphysical composition of clouds. One well-understood effect is that the ingestion of additional aerosols in warm (i.e., liquid) clouds could increase cloud droplet number, which enhance cloud reflectance and radiatively cool the surface - referred to as the "Twomey effect" [*Twomey*, 1977]. In addition, aerosol-induced microphysical changes may alter the subsequent microphysical, thermodynamic, and dynamic processes in clouds and their interactions with the ambient atmosphere, leading to diverse responses in the evolution of clouds and precipitation [*Albrecht*, 1989; *Rosenfeld*, 1999]. For example, observations of individual deep convective clouds (DCCs) polluted by aerosols often reported higher cloud tops, greater cloud cover, and invigorated convections [*Andreae et al.*, 2004; *Rosenfeld et al.*, 2008; *Li et al.*, 2011; *Niu and Li*, 2012; *Chen et al.*, 2016]. These observed responses to aerosols have been attributed to the release of latent heat at higher altitudes [*Rosenfeld et al.*, 2008] or the slowed dissipation of the anvil of DCCs [*Fan et al.*, 2013]. Subsequent processes in individual DCCs can lead to either enhancement or suppression of convective rainfall in response to aerosols [e.g., *Khain et al.*, 2005; *Tao et al.*, 2007; *Lebo and Morrison*, 2014; *Fan et al.*, 2018].

The impacts of aerosols on mesoscale convective systems (MCSs) are poorly understood [*Fan et al.*, 2016]. MCSs are highly organized convective systems extending more than 100 km in at least one direction, including regions of both convective and stratiform precipitation and are often responsible for heavy precipitation [*Houze*, 2004]. Studies have found that the responses of individual MCSs to aerosols differ by the type of MCSs, by the stages of the MCSs within their life cycles, and may be non-monotonic to aerosol abundance [e.g., *Khain et al.*, 2005; *Tao et al.*, 2007; *Li et al.*, 2009; *Lebo and Morrison*, 2014; *Kawecki et al.*, 2016; *Chakraborty et al.*, 2018; *Clavner et al.*, 2018; *Fan et al.*, 2018], but there is currently no holistic theory to explain these diverse responses [e.g., *Stevens and Feingold*, 2009; *Tao et al.*, 2012; *Fan et al.*, 2016]. An important reason for the diverse responses of MCSs to aerosols is likely related to the variety of environments and synoptic-scale weather systems in which MCSs are embedded [*Houze et al.*, 2015]. Previous studies mostly focused on the impacts of aerosols on individual MCSs. Much less is known about how aerosols perturb the interactions between the MCS and its ambient atmosphere to ultimately affect the climatology of MCSs.

Over Southern China, precipitation in late spring (April and May), prior to the onset of East Asian Summer Monsoon, has decreased significantly between the late 1970s and the 2000s [*Yang and Lau*, 2004; *Liu et al.*, 2005; *Xin et al.*, 2006; *Qiu et al.*, 2009; *Gemmer et al.*, 2011; *Zhu et al.*, 2014; *Day et al.*, 2018; *Li et al.*, 2018; *You and Jia*, 2018], in contrast to the better-known positive trends of summer and annual precipitation over this region [e.g., *Zhai et al.*, 2005; *Ding et al.*, 2007]. Several studies have tentatively linked the decreasing springtime precipitation over Southern China to interdecadal climate variability [*Yang and Lau*, 2004; *Xin et al.*, 2006; *Qiu et al.*, 2009; *Zhu et al.*, 2014; *You and Jia*, 2018]. However, concurrent with the decline in springtime precipitation, Chinese anthropogenic emission of aerosols and their precursors have approximately doubled between the late 1970s and the late 2000s [*Lamarque et al.*, 2010], and surface aerosol extinction coefficients over Southern China have significantly increased [*J. Li et al.*, 2016]. Given that approximately 90% of the total rainfall over Southern China in late spring is attributable to MCSs [*Luo et al.*, 2013], it is possible that the responses of MCSs to increasing aerosols may have contributed to the decline of late-spring precipitation. A few modeling studies have investigated the impacts of aerosols to late-spring precipitation over Southern China [*Kim et al.*, 2007; *Liu et al.*, 2011; *Hu and Liu*, 2013; *Jiang et al.*, 2015], but these previous studies used coarse-resolution climate models that were unable to explicitly characterize the impacts of aerosols to MCSs.

In this study, we used observations and simulations to explore the impacts of aerosols on both the MCSs and the environment from whence MCSs occur. We focused on the month of April (the beginning of the raining season in Southern China) to highlight the impacts on MCSs while avoiding confounding signals from the East Asian Summer Monsoon and the Meiyu fronts, both on-setting in May [*Luo et al.*, 2013; *Day et al.*, 2018].

2 Observed changes in April precipitation over Southern China during the recent decades

We first examined the changes in rainfall and rainfall intensities over Southern China for the month of April during recent decades. Figure 1a shows that April precipitation over Southern China during the more polluted period of 2001-2011 has decreased relative to that during the cleaner period of 1979-1989 according to the Global Precipitation Climatology Project (GPCP) dataset [*Adler et al.*, 2003], consistent with the findings of previous observational analyses [e.g., *Li et al.*, 2018; *You and Jia*, 2018]. Figure 1b shows the time series of April precipitation over Southern China between 1979 and 2015 from the GPCP dataset. There is a general negative trend in precipitation (-16.8±3.0 mm decade^{-1}, p-value = 0.017) during this period despite the large interannual variability. The mean April precipitation during the more polluted periods of 2001-2011 was 128.3±10.1 mm, significantly lower (p-value = 0.004) than the 170.4±10.5 mm during the cleaner period of 1979-1989. A similar reduction was also found from the surface rain gauge data (Figure S1). Measurements at 59 surface stations (Figure 1c) showed that the decline in precipitation during the polluted period relative to the clean period was due to decreased strong rainfall. Interestingly, Figure

1b showed that the decline of April precipitation over Southern China was evident during the 1980s and 2000s but not so during the 1990s. *J. Li et al.* [2016] analyzed surface visibility observations and found that the surface aerosol extinction coefficients over Southern China increased sharply during the 1980s and 2000s but declined slightly during the 1990s. These observations are qualitative consistent with our hypothesis that increased levels of aerosols may have affected springtime MCS activities over Southern China, leading to reduced precipitation. We investigated with model simulations below.

3 Simulated impacts of anthropogenic aerosols on rainfall and MCSs over Southern China in April

We used the Weather Research and Forecasting model coupled to Chemistry (WRF-Chem) [*Grell et al.*, 2005] to simulate April precipitation over Southern China for the years 2009 and 2010. Our model setup is described in the supporting information. Briefly, radiative scattering/absorption by aerosol and clouds were explicitly calculated using aerosol and cloud optical thicknesses [*Chou and Suarez*, 1994]. Cloud microphysics were simulated using a two-moment bulk scheme [*Morrison et al.*, 2005, 2009], while CCN-activation was simulated using the κ-Köhler theory [*Petters and Kreidenweis*, 2007]. *Fan et al.* [2012, 2015] previously showed that, when coupled to prognostic CCN-activation, the Morrison two-moment scheme was able to simulate the RADAR reflectivity of deep convections, and its simulated sensitivity of hydrometers to aerosols was similar to that simulated by a spectral bin microphysics scheme. The default IN-activation scheme in WRF-Chem was dependent solely on temperature but not on aerosols. We modified the IN scheme to include dependency on particle number [*DeMott et al.*, 2010] but found that this modification had little impact on our main conclusions (Figure S3).

We conducted pairs of sensitivity simulations by including and excluding Chinese emissions of anthropogenic aerosols and precursors to represent polluted and clean conditions, respectively. We simulated the years 2009 and 2010 to qualify the interannual variability while also avoiding the potential confounding influences of the sharp reduction in Chinese anthropogenic emissions since 2013 [e.g., *Li et al.*, 2017; *Zheng et al.*, 2018]. We verified that the polluted simulations reproduced the observed regional climatological features of rainfall and aerosols over Southern China (Text S1 and Figure S4).

We found that the accumulated April precipitation over Southern China in the polluted simulations were 16% and 8% lower than those in the clean simulations for 2009 and 2010, respectively (Figure S5). In addition, the PDFs of rainfall intensity showed less heavy rain in the polluted simulations relative to the clean simulations (Figure 2a). These model results were qualitatively consistent with the observed decreases in April rainfall over Southern China during the past decades as the region became more polluted (Figure 1). We found that more than 70% (for 2009) and 90% (for 2010) of the April precipitation reduction between the polluted and clean simulations occurred within the convective areas (defined as maximum RADAR reflectivity in the vertical column ⩾35 dBZ, Figure S6).

We next examined the impacts of aerosol pollution on MCS activities over Southern China in April. We developed an automated algorithm to objectively detect the occurrences and spatial extents of MCSs in our simulations based on the definition of MCSs [*Parker and Johnson*, 2000]. We defined the occurrence of an MCS as the presence of a strictly contiguous surface area satisfying the following criteria: (1) all surface grids within the area has RADAR reflectivity ⩾40 dBZ somewhere in the vertical column of air above it; (2) some model grids within that contiguous area have ⩾45 dBZ RADAR reflectivity; (3) the contiguous area extends ⩾100 km in at least one horizontal direction (4) but extends ⩽250 km in all horizontal directions.

Figure 2b shows the total number-hours of MCS occurrences in our simulations for April 2009 and April 2010, parsed from hourly model outputs using our automated algorithm. For April 2009, the total number-hours of MCS occurrences decreased from 689 hours under clean conditions to 471 hours under polluted conditions (-32%). Similarly, the total number-hours of MCS occurrences decreased from 962 hours under clean conditions to 756 hours under polluted conditions in April 2010 (-21%). This reduction in MCS occurrences in polluted simulations relative to clean simulations was not affected by changes in the thresholds used in the automated algorithm (Text S2). We further found that the reduced number-hours of MCSs under polluted conditions was not due to a shortening of individual MCS lifetime (Figure S7a), or a reduction in the horizontal extent of individual MCSs (Figure S7b), nor a reduction of rainfall intensity from individual MCSs (Figure S7c). In addition, the simulated reduction in total monthly precipitation over Southern China under polluted conditions was mainly driven by reduction in the monthly MCS rainfall (Figure S8). In fact, there was a slight increase in the monthly non-MCS rainfall under polluted conditions (Figure S8). We thus concluded that higher concentrations of anthropogenic aerosols suppressed the number of MCSs that occurred, leading to less total rainfall and weaker rainfall intensity over Southern China in April. Sensitivity experiments showed that the use of aerosol number-dependent IN-activation did slightly impact the simulated rainfall intensity, but it did not affect our main finding that higher levels of aerosols suppressed MCS occurrences (Figure S3).

We also examined the impacts of aerosols on the simulated structure of individual MCSs. The results were consistent with previous observations and model studies: for each individual MCS that occurred, increased aerosols led to a stronger and deeper convective core [e.g., *Rosenfeld et al.*, 2008; *Lee et al.*, 2016; *Guo et al.*, 2016]. Figure 3 shows the composite normalized contoured frequency of RADAR reflectivity as a function of altitude [*Yuter and Houze*, 1995; Text S3] for all simulated MCSs for April 2009 under polluted and clean conditions, as well as the difference between the two conditions. The MCSs simulated under polluted conditions had stronger convective cores (RADAR reflectivity $\geqslant$40 dBZ) that also developed to higher altitudes. Below

1 km, the RADAR reflectivity under the MCSs shifted slightly toward smaller values under polluted conditions due to an 8.7% radius-reduction of raindrops, which likely evaporated more quickly. Overall, the RADAR reflectivity of MCSs under polluted conditions was invigorated at midlevel and shifted toward lower values near the surface (Figure 3c), consistent with observations [*Guo et al.*, 2018]. However, the rainfall reaching the surface from individual MCSs was not significantly different in the polluted and clean simulations (Figure S7c).

4 Mechanisms by which aerosol suppresses MCS occurrences

We analyzed the impacts of aerosols on the simulated radiative and thermodynamic conditions over Southern China (Tables 1 and S2) to diagnose the mechanism by which aerosol suppresses MCS occurrences. Over land areas in Southern China in April 2009, the simulated air temperature and downward shortwave flux at surface under polluted conditions were 0.5 ^{o}C cooler and 24 W m^{-2} lower than those under clean conditions, respectively (Table 1). The simulated domain-average convective available potential energy (CAPE) under polluted conditions was 17% lower than that under clean conditions. Similar simulated changes were found for April 2010 (Table S2). These findings suggested that anthropogenic aerosols may suppress MCS occurrence in part by cooling the surface air and increasing regional atmospheric stability.

We found that in the polluted simulations, the domain-average aerosol optical depth (AOD) were 0.34 and 0.39 over Southern China for 2009 and 2010 (Tables 1 and S2), respectively, which was ten and six times higher than those in the clean simulations, respectively. The ingestion of additional anthropogenic aerosols by warm clouds led to the domain-average liquid cloud droplet numbers in the polluted simulations to be approximately four times the values in the clean simulations (Table S3). The cloud liquid water content below 750 hPa in the polluted simulations were 38% higher than that in the clean simulations (Table S3). As a result, the domain-averaged liquid cloud optical thicknesses (LCOT) in the lower troposphere in the polluted simulations were approximately twice of the values in the clean simulations for April 2009 and 2010 (Tables 1 and S2). In other words, under polluted conditions, more aerosols were activated into more numerous liquid cloud droplets and the cloud liquid water contents were larger (Table S3), both contributing to larger LCOT. This is the “Twomey effect” of aerosols on warm clouds. We found that the warm cloud coverage over Southern China in April was extensive (46% over our simulated domain) and was mainly associated with the frontal systems in which the MCSs were embedded. Only 0.4%-0.6% of the warm cloud coverage was directly associated with the MCSs themselves, based on the delineation of MCSs (Section 3). Thus, the Twomey effect of aerosols was mainly manifested by the non-MCS warm clouds. It thus appeared that either the direct radiative effect or the Twomey effect of aerosols, or the combination of these two effects, may be effectively cooling the surface and increasing regional atmospheric stability.

We designed further sensitivity simulations to elucidate the mechanisms by which aerosols suppress MCS occurrences over Southern China. First, we turned off the direct radiative forcings of aerosols while keeping all other model configurations the same as those in the polluted simulations for April 2009 and April 2010 ("Polluted_NoADE" simulations). We found that, by turning off the direct radiative forcing of aerosols, the number-hour of MCS increased (from 471 to 538 for April 2009 and from 756 to 776 for April 2010, Figure 2b), the accumulated rainfall increased (Figure S5), and the rainfall intensities shifted toward heavier rainfall (Figure 2a), relative to the base polluted case. However, the changes were not enough to explain the large differences between the clean and polluted simulations.

Secondly, we repeated the polluted simulations for April 2009 and April 2010 but decreased the LCOT values by 50% in the radiation calculation only ("Polluted_0.5LCOT" simulations). In these simulations, the number-hour of MCS activities (increased from 471 to 584 for April 2009 and from 756 to 804 for April 2010, Figure 2b), the accumulated rainfall (Figure S5), and the rainfall intensity (Figure 2a) all increased significantly relative to the base polluted case, and they were both closer to the values in the clean simulations than those in the "Polluted_NoADE" simulations. This suggested that the Twomey effect of aerosols, which mostly involved the non-MCS warm clouds, played a stronger role than the aerosol direct radiative effect in suppressing MCS occurrences over Southern China in April.

Finally, we conducted simulations where the direct radiative forcing of aerosols was turned off and the LCOT used in radiative calculations were halved ("Polluted_0.5LCOT_NoADE" simulations). This was equivalent to shutting off both the direct radiative forcing and the Twomey effect of aerosols on warm clouds. The simulated MCS activities increased significantly relative to the base polluted simulation (from 471 to 574 for April 2009 and from 756 to 851 for April 2010, Figure 2b). The accumulated rainfall and rainfall intensity both increased (Figures S5 and 2a). Combined, the direct effect and Twomey effect of aerosols acting on ambient atmosphere accounted for approximately half of the total MCS occurrence suppression due to anthropogenic aerosols (Figure 2b).

Tables 1 and S2 diagnosed the simulated thermodynamic variables in the sensitivity simulations over Southern China land areas for April 2009 and 2010. Relative to the base polluted simulations, if the direct radiative forcing and the Twomey effect of aerosols on warm clouds were turned off, either individually or combined, the simulated thermodynamic conditions would become more conducive to MCS occurrences. The direct and Twomey effects of aerosols enhanced atmospheric stability and reduced CAPE by cooling surface air. Although individual MCSs polluted by anthropogenic aerosols showed stronger convective cores (Section 3 and Figure 3), the overall numbers of MCSs were reduced under polluted conditions relative to clean conditions. As a result, for the entire Southern China, the domain-average cloud top temperature was higher (i.e., lower average cloud top height) and the updraft velocity were lower under polluted conditions, indicating less convective activities in the region overall. Furthermore, the simulated moisture convergence in the boundary layer and the precipitable water over Southern China were also reduced under polluted conditions, suggesting a possible feedback between regional convection and large-scale moisture convergence [*Li et al.*, 2018].

Our result also indicated that, in addition to the direct and Twomey effects of aerosols, subsequent aerosol-induced microphysical, thermodynamic, and dynamic changes of MCS and the ambient atmosphere led to the other half of the MCS suppression by aerosols (differences between the blue and green bars in Figure 2b).

5 Conclusions

Based on our observational analyses and model simulations, we constructed a conceptual model (Figure 4) to elucidate the impacts of aerosols on MCS occurrences and precipitation over Southern China in April. Under clean conditions (Figure 4a), MCSs embedded in frontal systems are triggered by the unstable surface atmosphere and dynamic conditions [*Luo et al.*, 2013]. Under polluted conditions (Figure 4b), increased concentrations of aerosols enhance direct radiative scattering. The ingestion of more aerosols in non-MCS warm clouds also lead to higher warm cloud reflectance via the Twomey effect. Both of these effects stabilize the atmosphere and suppress MCS occurrences. Subsequent microphysical, thermodynamic, and dynamic adjustment lead to further reduction in MCS occurrences. Meanwhile, the precipitation from and the lifetimes and sizes of individual MCS that did occur were not significantly altered by aerosols. The reduced MCS occurrences under polluted conditions result in less accumulated precipitation and weaker rainfall intensity. This suppression of aerosols on MCS occurrences contributed to the observed declining late spring precipitation over Southern China in recent decades, although the interdecadal variability of climate likely also played a role.

MCSs over Southern China in April are mostly associated with frontal systems [*Luo et al.*, 2013; *Day et al.*, 2018] with extensive warm cloud coverages. Hence there is great leverage for the Twomey effect of aerosols on warm clouds to stabilize the regional atmosphere. MCSs associated with other synoptic weather systems, such as the summertime MCSs triggered by local instability [*Ding and Chan*, 2005] or convergence preceding landfalling tropical cyclones [*Meng and Zhang*, 2012], may be accompanied by less warm clouds, with less leverage for Twomey effect. This may explain why previous studies on summertime MCSs and rainfall over Southern China generally found increased precipitation under polluted conditions relative to clean conditions [e.g., *Z. Li et al.*, 2016; *Guo et al.*, 2017].

Our results indicate that the impacts of aerosols on the thermodynamic environment from whence the MCS develop, can be important pathways by which aerosols affect MCSs. Moreover, the traditional view of separating the aerosol-cloud interactions for warm and convective clouds does not work, as adjustments happen not only in each cloud system in isolation, but also between different cloud systems via interactions with the regional atmosphere, as shown here. Future model studies should simulate synoptic-scale spatial domains and for longer periods to elucidate the full impacts of aerosols on MCSs and the associated precipitation.

Acknowledgements

This study was funded by the National Natural Science Foundation of China (41461164007, 41975158). The surface rain gauge data (https://gis.ncdc.noaa.gov/maps/ncei) and the GPCP dataset (version 2.3, https://www.esrl.noaa.gov/psd/data/gridded/data.gpcp.html) are freely available from the National Oceanic and Atmospheric Administration (NOAA). The NCEP FNL Operational Global Analysis data is freely available from the National Center for Atmospheric Research (https://rda.ucar.edu/datasets/). Anthropogenic emissions of aerosols and precursors for China (http://www.meicmodel.org) and for the rest of Asia (https://espo.nasa.gov/intex-b) are available online and from the developers. Our WRF-Chem model metadata and outputs are archived at https://opendata.pku.edu.cn/dataverse/atmoschem/.

References

Ackermann, I. J., H. Hass, M. Memmesheimer, A. Ebel, F. S. Binkowski, and U. Shankar (1998), Modal aerosol dynamics model for Europe: Development and first applications, *Atmos. Environ.*, *32*(17), 2981-2999, doi:10.1016/s1352-2310(98)00006-5.

Adler, R. F., et al. (2003), The version-2 global precipitation climatology project (GPCP) monthly precipitation analysis (1979-present), *J. Hydrometeorol.*, *4*(6), 1147-1167, doi:10.1175/1525-7541(2003)004<1147:tvgpcp>2.0.co;2

Albrecht, B. A. (1989), Aerosols, Cloud Microphysics, and Fractional Cloudiness, *Science*, *245*(4923), 1227-1230, doi:10.1126/science.245.4923.1227.

Andreae, M. O., D. Rosenfeld, P. Artaxo, A. A. Costa, G. P. Frank, K. M. Longo, and M. A. F. Silva-Dias (2004), Smoking rain clouds over the Amazon, *Science*, *303*(5662), 1337-1342, doi:10.1126/science.1092779.

Chakraborty, S., R. Fu, D. Rosenfeld, and S. T. Massie (2018), The Influence of Aerosols and Meteorological Conditions on the Total Rain Volume of the Mesoscale Convective Systems Over Tropical Continents, *Geophys. Res. Lett.*, *45*(23), 13099-13106, doi:10.1029/2018gl080371.

Chen, T., J. Guo, Z. Li, C. Zhao, H. Liu, M. Cribb, F. Wang, and J. He (2016), A CloudSat Perspective on the Cloud Climatology and Its Association with Aerosol Perturbations in the Vertical over Eastern China, *J. Atmos. Sci.*, *73*(9), 3599-3616, doi:10.1175/jas-d-15-0309.1.

Chou, M.-D., and M. J. Suarez (1994), *An Efficient Thermal Infrared Radiation Parameterization for Use in General Circulation Models*, NASA Technical Memorandum No. 104606, Vol.3, 85p. https://archive.org/details/nasa_techdoc_19950009331.

Clavner, M., W. R. Cotton, S. C. van den Heever, S. M. Saleeby, and J. R. Pierce (2018), The response of a simulated mesoscale convective system to increased aerosol pollution: Part I: Precipitation intensity, distribution, and efficiency, *Atmos. Res.*, *199*, 193-208, doi:10.1016/j.atmosres.2017.08.010.

Day, J. A., I. Fung, and W. Liu (2018), Changing character of rainfall in eastern China, 1951-2007, *Proc. Natl. Acad. Sci. USA*, *115*(9), 2016-2021, doi:10.1073/pnas.1715386115.

DeMott, P. J., A. J. Prenni, X. Liu, S. M. Kreidenweis, M. D. Petters, C. H. Twohy, M. S. Richardson, T. Eidhammer, and D. C. Rogers (2010), Predicting global atmospheric ice nuclei distributions and their impacts on climate, *Proc. Natl. Acad. Sci. USA*, *107*(25), 11217-11222, doi:10.1073/pnas.0910818107.

Ding, Y., and J. C. L. Chan (2005), The East Asian summer monsoon: an overview, *Meteorol. Atmos. Phys.*, *89*(1-4), 117-142, doi:10.1007/s00703-005-0125-z.

Ding, Y., G. Ren, Z. Zhao, Y. Xu, Y. Luo, Q. Li, and J. Zhang (2007), Detection, causes and projection of climate change over China: An overview of recent progress, *Adv. Atmos. Sci.*, *24*(6), 954-971, doi:10.1007/s00376-007-0954-4.

Emmons, L. K., et al. (2010), Description and evaluation of the Model for Ozone and Related chemical Tracers, version 4 (MOZART-4), *Geosci. Model Dev.*, *3*(1), 43-67, doi:10.5194/gmd-3-43-2010.

Fan, J., L. R. Leung, Z. Q. Li, H. Morrison, H. B. Chen, Y. Q. Zhou, Y. Qian, and Y. Wang (2012), Aerosol impacts on clouds and precipitation in eastern China: Results from bin and bulk microphysics, *J. Geophys. Res. Atmos.*, *117*, 21, doi:10.1029/2011jd016537.

Fan, J., L. R. Leung, D. Rosenfeld, Q. Chen, Z. Li, J. Zhang, and H. Yan (2013), Microphysical effects determine macrophysical response for aerosol impacts on deep convective clouds, *Proc. Natl. Acad. Sci. USA*, *110*(48), 4581-4590, doi:10.1073/pnas.1316830110.

Fan, J., Y. Liu, K. Xu, K. North, S. Collis, X. Dong, G. Zhang, Q. Chen, P. Kollias, and S. J. Ghan (2015), Improving representation of convective transport for scale-aware parameterization: 1. Convection and cloud properties simulated with spectral bin and bulk microphysics, *J. Geophys. Res. Atmos.*, *120*(8), 3485-3509, doi:10.1002/2014jd022142.

Fan, J., Y. Wang, D. Rosenfeld, and X. Liu (2016), Review of Aerosol-Cloud Interactions: Mechanisms, Significance, and Challenges, *J. Atmos. Sci.*, *73*(11), 4221-4252, doi:10.1175/jas-d-16-0037.1.

Fan, J., et al. (2018), Substantial convection and precipitation enhancements by ultrafine aerosol particles, *Science*, *359*(6374), 411-418, doi:10.1126/science.aan8461.

Gemmer, M., T. Fischer, T. Jiang, B. Su, and L. L. Liu (2011), Trends in Precipitation Extremes in the Zhujiang River Basin, South China, *J. Clim.*, *24*(3), 750-761, doi:10.1175/2010jcli3717.1.

Grell, G. A., S. E. Peckham, R. Schmitz, S. A. McKeen, G. Frost, W. C. Skamarock, and B. Eder (2005), Fully coupled "online" chemistry within the WRF model, *Atmos. Environ.*, *39*(37), 6957-6975, doi:10.1016/j.atmosenv.2005.04.027.

Guenther, A., T. Karl, P. Harley, C. Wiedinmyer, P. I. Palmer, and C. Geron (2006), Estimates of global terrestrial isoprene emissions using MEGAN (Model of Emissions of Gases and Aerosols from Nature), *Atmos. Chem. Phys.*, *6*, 3181-3210, doi:10.5194/acp-6-3181-2006.

Guo, J., M. J. Deng, S. S. Lee, F. Wang, Z. Q. Li, P. M. Zhai, H. Liu, W. T. Lv, W. Yao, and X. W. Li (2016), Delaying precipitation and lightning by air pollution over the Pearl River Delta. Part I: Observational analyses, *J. Geophys. Res. Atmos.*, *121*(11), 6472-6488, doi:10.1002/2015jd023257.

Guo, J., T. Su, Z. Li, Y. Miao, J. Li, H. Liu, H. Xu, M. Cribb, and P. Zhai (2017), Declining frequency of summertime local-scale precipitation over eastern China from 1970 to 2010 and its potential link to aerosols, *Geophys. Res. Lett.*, *44*(11), 5700-5708, doi:10.1002/2017gl073533.

Guo, J., et al. (2018), Aerosol-induced changes in the vertical structure of precipitation: a perspective of TRMM precipitation radar, *Atmos. Chem. Phys.*, *18*(18), 13329-13343, doi:10.5194/acp-18-13329-2018.

Hansen, J., M. Sato, and R. Ruedy (1997), Radiative forcing and climate response, *J. Geophys. Res. Atmos.*, *102*(D6), 6831-6864, doi:10.1029/96jd03436.

Houze, R. A. (2004), Mesoscale convective systems, *Rev. Geophys.*, *42*(4), RG4003, doi:10.1029/2004rg000150.

Houze, R. A., Jr., K. L. Rasmussen, M. D. Zuluaga, and S. R. Brodzik (2015), The variable nature of convection in the tropics and subtropics: A legacy of 16 years of the Tropical Rainfall Measuring Mission satellite, *Rev. Geophys.*, *53*(3), 994-1021, doi:10.1002/2015rg000488.

Hu, N., and X. Liu (2013), Modeling Study of the Effect of Anthropogenic Aerosols on Late Spring Drought in South China, *Acta. Meteorol. Sin.*, *27*(5), 701-715, doi:10.1007/s13351-013-0506-z.

Huang, X. F., C. Wang, J. F. Peng, L. Y. He, L. M. Cao, Q. Zhu, J. Cui, Z. J. Wu, and M. Hu (2017), Characterization of particle number size distribution and new particle formation in Southern China, *J. Environ. Sci.*, *51*, 342-351, doi:10.1016/j.jes.2016.05.039.

Intergovernmental Panel on Climate Change (IPCC) (2013), *Climate Change 2013: The Physical Science Basis. Contribution of Working Group I to the Fifth Assessment Report of the Intergovernmental Panel on Climate Change*, edited by T. F. Stocker et al., pp. 1535, Cambridge Univ. Press, Cambridge, U. K., and New York.

Jiang, Y., X.-Q. Yang, and X. Liu (2015), Seasonality in anthropogenic aerosol effects on East Asian climate simulated with CAM5, *J. Geophys. Res. Atmos.*, *120*(20), 10837-10861, doi:10.1002/2015jd023451.

Kawecki, S., G. M. Henebry, and A. L. Steiner (2016), Effects of Urban Plume Aerosols on a Mesoscale Convective System, *J. Atmos. Sci.*, *73*(12), 4641-4660, doi:10.1175/jas-d-16-0084.1.

Khain, A., D. Rosenfeld, and A. Pokrovsky (2005), Aerosol impact on the dynamics and microphysics of deep convective clouds, *Q. J. R. Meteorol. Soc.*, *131*(611), 2639-2663, doi:10.1256/qj.04.62.

Kim, M.-K., W. K. M. Lau, K.-M. Kim, and W.-S. Lee (2007), A GCM study of effects of radiative forcing of sulfate aerosol on large scale circulation and rainfall in East Asia during boreal spring, *Geophys. Res. Lett.*, *34*(24), L24701, doi:10.1029/2007gl031683.

Lai, S. C., Y. Zhao, A. J. Ding, Y. Y. Zhang, T. L. Song, J. Y. Zheng, K. F. Ho, S. C. Lee, and L. J. Zhong (2016), Characterization of PM2.5 and the major chemical components during a 1-year campaign in rural Guangzhou, Southern China, *Atmos. Res.*, *167*, 208-215, doi:10.1016/j.atmosres.2015.08.007.

Lamarque, J. F., et al. (2010), Historical (1850-2000) gridded anthropogenic and biomass burning emissions of reactive gases and aerosols: methodology and application, *Atmos. Chem. Phys.*, *10*(15), 7017-7039, doi:10.5194/acp-10-7017-2010.

Lebo, Z. J., and H. Morrison (2014), Dynamical Effects of Aerosol Perturbations on Simulated Idealized Squall Lines, *Mon. Weather Rev.*, *142*(3), 991-1009, doi:10.1175/mwr-d-13-00156.1.

Lee, S. S., J. P. Guo, and Z. Q. Li (2016), Delaying precipitation by air pollution over the Pearl River Delta: 2. Model simulations, *J. Geophys. Res. Atmos.*, *121*(19), 11739-11760, doi:10.1002/2015jd024362.

Li, C., et al. (2017), India Is Overtaking China as the World's Largest Emitter of Anthropogenic Sulfur Dioxide, *Sci. Rep.*, *7*, 7, doi:10.1038/s41598-017-14639-8.

Li, G., Y. Wang, K.-H. Lee, Y. Diao, and R. Zhang (2009), Impacts of aerosols on the development and precipitation of a mesoscale squall line, *J. Geophys. Res. Atmos.*, *114*, 209-214, doi:10.1029/2008jd011581.

Li, J., C. C. Li, C. S. Zhao, and T. N. Su (2016), Changes in surface aerosol extinction trends over China during 1980-2013 inferred from quality-controlled visibility data, *Geophys. Res. Lett.*, *43*(16), 8713-8719, doi:10.1002/2016gl070201.

Li, P., T. Zhou, and X. Chen (2018), Water vapor transport for spring persistent rains over southeastern China based on five reanalysis datasets, *Clim. Dyn.*, *51*(11-12), 4243-4257, doi:10.1007/s00382-017-3680-3.

Li, Z., F. Niu, J. W. Fan, Y. G. Liu, D. Rosenfeld, and Y. N. Ding (2011), Long-term impacts of aerosols on the vertical development of clouds and precipitation, *Nature Geosci.*, *4*(12), 888-894, doi:10.1038/ngeo1313.

Li, Z., et al. (2016), Aerosol and monsoon climate interactions over Asia, *Rev. Geophys.*, *54*(4), 866-929, doi:10.1002/2015rg000500.

Li, Z., et al. (2019), East Asian Study of Tropospheric Aerosols and their Impact on Regional Clouds, Precipitation, and Climate (EAST-AIR(CPC)), *J. Geophys. Res. Atmos.*, *124*(23), 13026-13054, doi:10.1029/2019jd030758.

Liu, B. H., M. Xu, M. Henderson, and Y. Qi (2005), Observed trends of precipitation amount, frequency, and intensity in China, 1960-2000, *J. Geophys. Res. Atmos.*, *110*(D8), D08103, doi:10.1029/2004jd004864.

Liu, F., Q. Zhang, D. Tong, B. Zheng, M. Li, H. Huo, and K. B. He (2015), High-resolution inventory of technologies, activities, and emissions of coal-fired power plants in China from 1990 to 2010, *Atmos. Chem. Phys.*, *15*(23), 13299-13317, doi:10.5194/acp-15-13299-2015.

Liu, X., X. Xie, Z.-Y. Yin, C. Liu, and A. Gettelman (2011), A modeling study of the effects of aerosols on clouds and precipitation over East Asia, *Theor. Appl. Clim.*, *106*(3-4), 343-354, doi:10.1007/s00704-011-0436-6.

Luo, Y., H. Wang, R. Zhang, W. Qian, and Z. Luo (2013), Comparison of Rainfall Characteristics and Convective Properties of Monsoon Precipitation Systems over South China and the Yangtze and Huai River Basin, *J. Clim.*, *26*(1), 110-132, doi:10.1175/jcli-d-12-00100.1.

Meng, Z., and Y. Zhang (2012), On the Squall Lines Preceding Landfalling Tropical Cyclones in China, *Mon. Weather Rev.*, *140*(2), 445-470, doi:10.1175/mwr-d-10-05080.1.

Morrison, H., J. A. Curry, and V. I. Khvorostyanov (2005), A new double-moment microphysics parameterization for application in cloud and climate models. Part I: Description, *J. Atmos. Sci.*, *62*(6), 1665-1677, doi:10.1175/jas3446.1.

Morrison, H., G. Thompson, and V. Tatarskii (2009), Impact of Cloud Microphysics on the Development of Trailing Stratiform Precipitation in a Simulated Squall Line: Comparison of One- and Two-Moment Schemes, *Mon. Weather Rev.*, *137*(3), 991-1007, doi:10.1175/2008mwr2556.1.

Niu, F., and Z. Li (2012), Systematic variations of cloud top temperature and precipitation rate with aerosols over the global tropics, *Atmos. Chem. Phys.*, *12*(18), 8491-8498, doi:10.5194/acp-12-8491-2012.

Parker, M. D., and R. H. Johnson (2000), Organizational modes of midlatitude mesoscale convective systems, *Mon. Weather Rev.*, *128*(10), 3413-3436, doi:10.1175/1520-0493(2001)129<3413:omommc>2.0.co;2.

Petters, M. D., and S. M. Kreidenweis (2007), A single parameter representation of hygroscopic growth and cloud condensation nucleus activity, *Atmos. Chem. Phys.*, *7*(8), 1961-1971, doi:10.5194/acp-7-1961-2007.

Qiu, Y., W. Cai, X. Guo, and A. Pan (2009), Dynamics of Late Spring Rainfall Reduction in Recent Decades over Southeastern China, *J. Clim.*, *22*(8), 2240-2247, doi:10.1175/2008jcli2809.1.

Rosenfeld, D. (1999), TRMM observed first direct evidence of smoke from forest fires inhibiting rainfall, *Geophys. Res. Lett.*, *26*(20), 3105-3108, doi:10.1029/1999gl006066.

Rosenfeld, D., U. Lohmann, G. B. Raga, C. D. O'Dowd, M. Kulmala, S. Fuzzi, A. Reissell, and M. O. Andreae (2008), Flood or drought: How do aerosols affect precipitation?, *Science*, *321*(5894), 1309-1313, doi:10.1126/science.1160606.

Schell, B., I. J. Ackermann, H. Hass, F. S. Binkowski, and A. Ebel (2001), Modeling the formation of secondary organic aerosol within a comprehensive air quality model system, *J. Geophys. Res. Atmos.*, *106*(D22), 28275-28293, doi:10.1029/2001jd000384.

Stevens, B., and G. Feingold (2009), Untangling aerosol effects on clouds and precipitation in a buffered system, *Nature*, *461*(7264), 607-613, doi:10.1038/nature08281.

Tao, J., L. M. Zhang, K. F. Ho, R. J. Zhang, Z. J. Lin, Z. S. Zhang, M. Lin, J. J. Cao, S. X. Liu, and G. H. Wang (2014), Impact of $PM_{2.5}$ chemical compositions on aerosol light scattering in Guangzhou - the largest megacity in South China, *Atmos. Res.*, *135*, 48-58, doi:10.1016/j.atmosres.2013.08.015.

Tao, W.-K., X. Li, A. Khain, T. Matsui, S. Lang, and J. Simpson (2007), Role of atmospheric aerosol concentration on deep convective precipitation: Cloud-resolving model simulations, *J. Geophys. Res. Atmos.*, *112*(D24), D24S18, doi:10.1029/2007jd008728.

Tao, W.-K., J.-P. Chen, Z. Li, C. Wang, and C. Zhang (2012), Impact of Aerosols on Convective Clouds and Precipitation, *Rev. Geophys.*, *50*, RG2001, doi:10.1029/2011rg000369.

Twomey, S. (1977), The Influece of Pollution on Shortwave Albedo of Clouds, *J. Atmos. Sci.*, *34*(7), 1149-1152, doi:10.1175/1520-0469(1977)034<1149:tiopot>2.0.co;2.

Wiedinmyer, C., S. K. Akagi, R. J. Yokelson, L. K. Emmons, J. A. Al-Saadi, J. J. Orlando, and A. J. Soja (2011), The Fire INventory from NCAR (FINN): a high resolution global model to estimate the emissions from open burning, *Geosci. Model Dev.*, *4*(3), 625-641, doi:10.5194/gmd-4-625-2011.

Xin, X., R. Yu, T. Zhou, and B. Wang (2006), Drought in late spring of South China in recent decades, *J. Clim.*, *19*(13), 3197-3206, doi:10.1175/jcli3794.1.

Yang, F. L., and K. M. Lau (2004), Trend and variability of China precipitation in spring and summer: Linkage to sea-surface temperatures, *Int. J. Climatol.*, *24*(13), 1625-1644, doi:10.1002/joc.1094.

You, Y., and X. Jia (2018), Interannual Variations and Prediction of Spring Precipitation over China, *J. Clim.*, *31*(2), 655-670, doi:10.1175/jcli-d-17-0233.1.

Yuter, S. E., and R. A. Houze (1995), Three-Dimensional Kinematic and Microphysical Evolution of Florida Cumulonimbus. Part II: Frequency Distributions of Vertical Velocity, Reflectivity, and Differential Refectivity, *Mon. Weather Rev.*, *123*(7), 1941-1963, doi:10.1175/1520-0493(1995)123<1941:tdkame>2.0.co;2.

Zhai, P. M., X. B. Zhang, H. Wan, and X. H. Pan (2005), Trends in total precipitation and frequency of daily precipitation extremes over China, *J. Clim.*, *18*(7), 1096-1108, doi:10.1175/jcli-3318.1.

Zhang, Q., et al. (2009), Asian emissions in 2006 for the NASA INTEX-B mission, *Atmos. Chem. Phys.*, *9*(14), 5131-5153, doi:10.5194/acp-9-5131-2009.

Zheng, B., et al. (2018), Trends in China's anthropogenic emissions since 2010 as the consequence of clean air actions, *Atmos. Chem. Phys.*, *18*(19), 14095-14111, doi:10.5194/acp-18-14095-2018.

Zhu, Z., T. Li, and J. He (2014), Out-of-Phase Relationship between Boreal Spring and Summer Decadal Rainfall Changes in Southern China, *J. Clim.*, *27*(3), 1083-1099, doi:10.1175/jcli-d-13-00180.1.

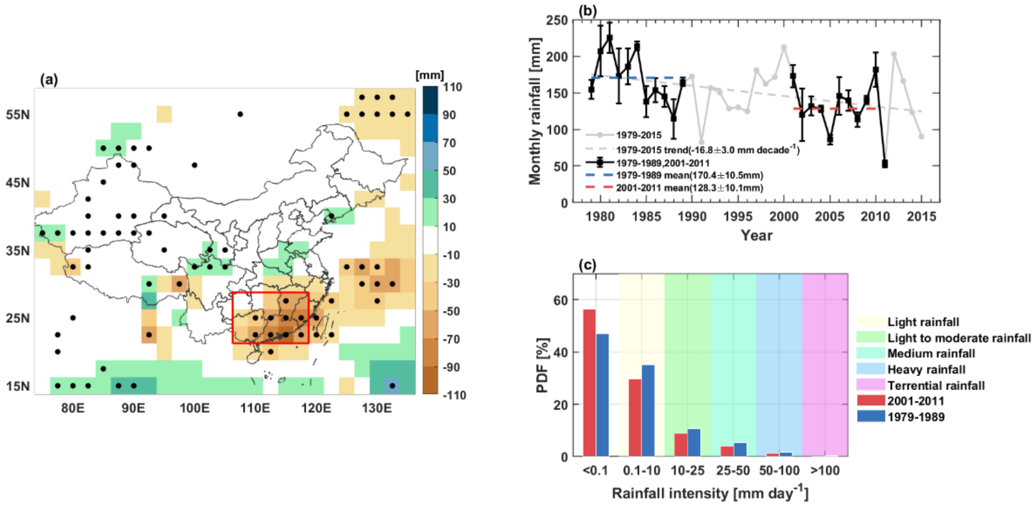

Figure 1. (a) Observed difference in April precipitation over China between the more polluted period of 2001-2011 versus the cleaner period of 1979-1989. Stilted grids indicate significant differences at the 90% confidence level. (b) Time series of April precipitation (grey solid line) over Southern China (red box in Figure 1a) between 1979 and 2015 and its linear trend (grey dashed line with the slope shown inset). The black line highlights the mean April precipitation during 1979 to 1989 and 2001 to 2011; the blue and red dashed lines indicate the mean during those periods, respectively. (c) Probability distribution of April daily rainfall intensity over Southern China during 1979 to 1989 (blue) and 2001 to 2011 (red) from surface gauge measurements. The categories of rainfall intensities, as defined by the Chinese Meteorological Administration, are shown in colors.

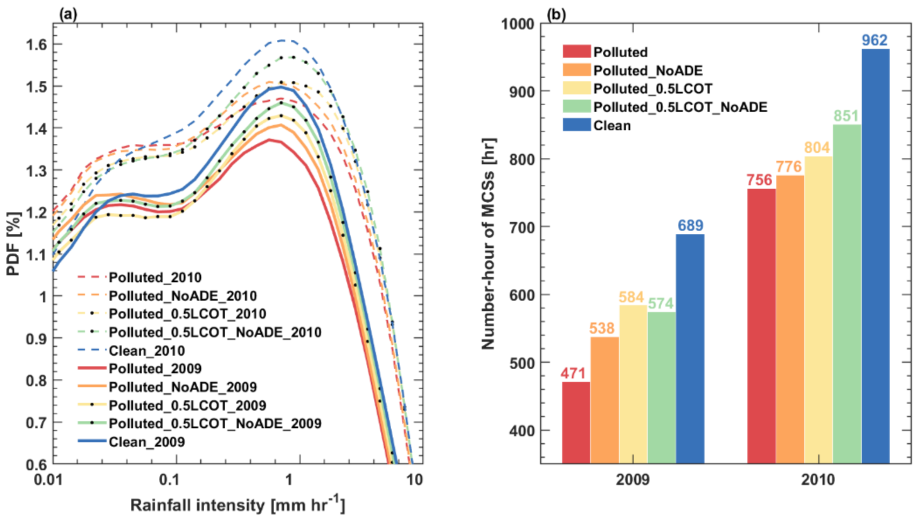

Figure 2. (a) Probability distribution functions of modelled rainfall intensity in the sensitivity simulations. Results from simulations for 2009 and 2010 are shown in solid and dashed lines, respectively. (b) The total number-hours of MCSs over Southern China in April parsed from the hourly model outputs of the sensitivity simulations. Color codes for the sensitivity simulations are shown inset.

594

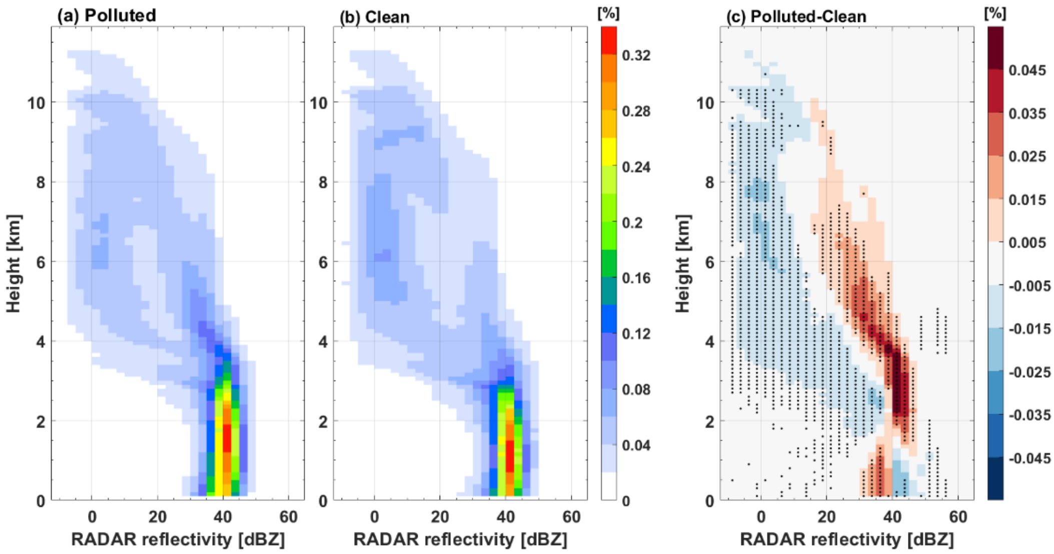

Figure 3. Composite of the normalized contoured frequency of RADAR reflectivity as a function of altitude for all simulated MCSs under (a) polluted conditions and (b) clean conditions in April 2009, respectively. Also shown is (c) the difference between (a) and (b). Stilted grids indicate significant differences at the 95% confidence level.

595

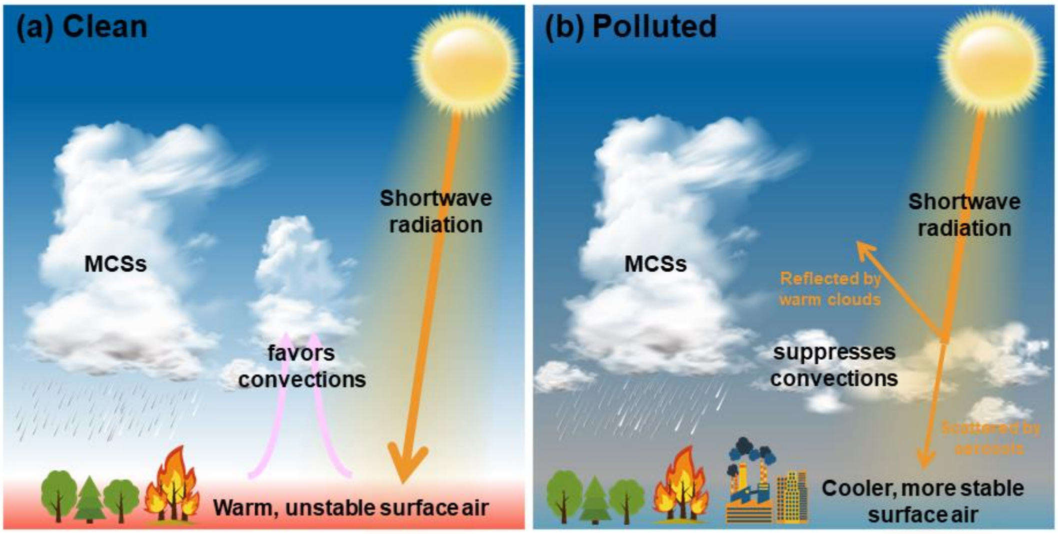

Figure 4. Schematic illustration of the impacts of anthropogenic aerosols on MCSs and precipitation over Southern China in April under (a) clean and (b) polluted conditions. Under polluted conditions, more aerosols lead to more direct scattering of solar radiation. Also, the ingestion of more aerosols in warm clouds leads enhanced cloud reflectance via the Twomey effect. Both of these effects stabilize the regional atmosphere and suppress MCS occurrences.

Table 1. Diagnostics of simulated surface and atmospheric thermodynamic variables in the sensitivity simulations for April 2009. Values are averages over the land areas in Southern China.

	Sensitivity simulations					
	Polluted	Polluted _NoADE	Polluted _0.5 LCOT	Polluted _NoADE _0.5 LCOT	Clean	**Percent impacts of aerosols (Polluted -Clean)/Polluted**
AOD (all sky)	0.343	0.326	0.325	0.309	0.0322	+90%
LCOT	62.6	63.4	30.0	30.6	31.25	+50%
April accumulated precipitation [mm]	256	263	273	281	297	-16%
Downward shortwave radiation at the surface [W m^{-2}]	201	206	213	214	225	-12%
T at 2 m [ºC]	20.2	20.3	20.5	20.6	20.7	-2.4%
Convective available potential energy (CAPE) [J]	277	277	285	286	323	-17%
Cloud top temperature [ºC]	-13.1	-14.0	-14.0	-14.9	-15.5	+18%
Vertical velocity [m s^{-1}]	0.0617	0.0629	0.0636	0.0649	0.0681	-10%
Moisture convergence [10^{-6} g cm^{-2} hPa^{-1} s^{-1}]	1.48	1.74	1.49	1.76	2.00	-36%
Precipitable water [mm]	36.3	36.4	36.4	36.5	36.7	-1.2%